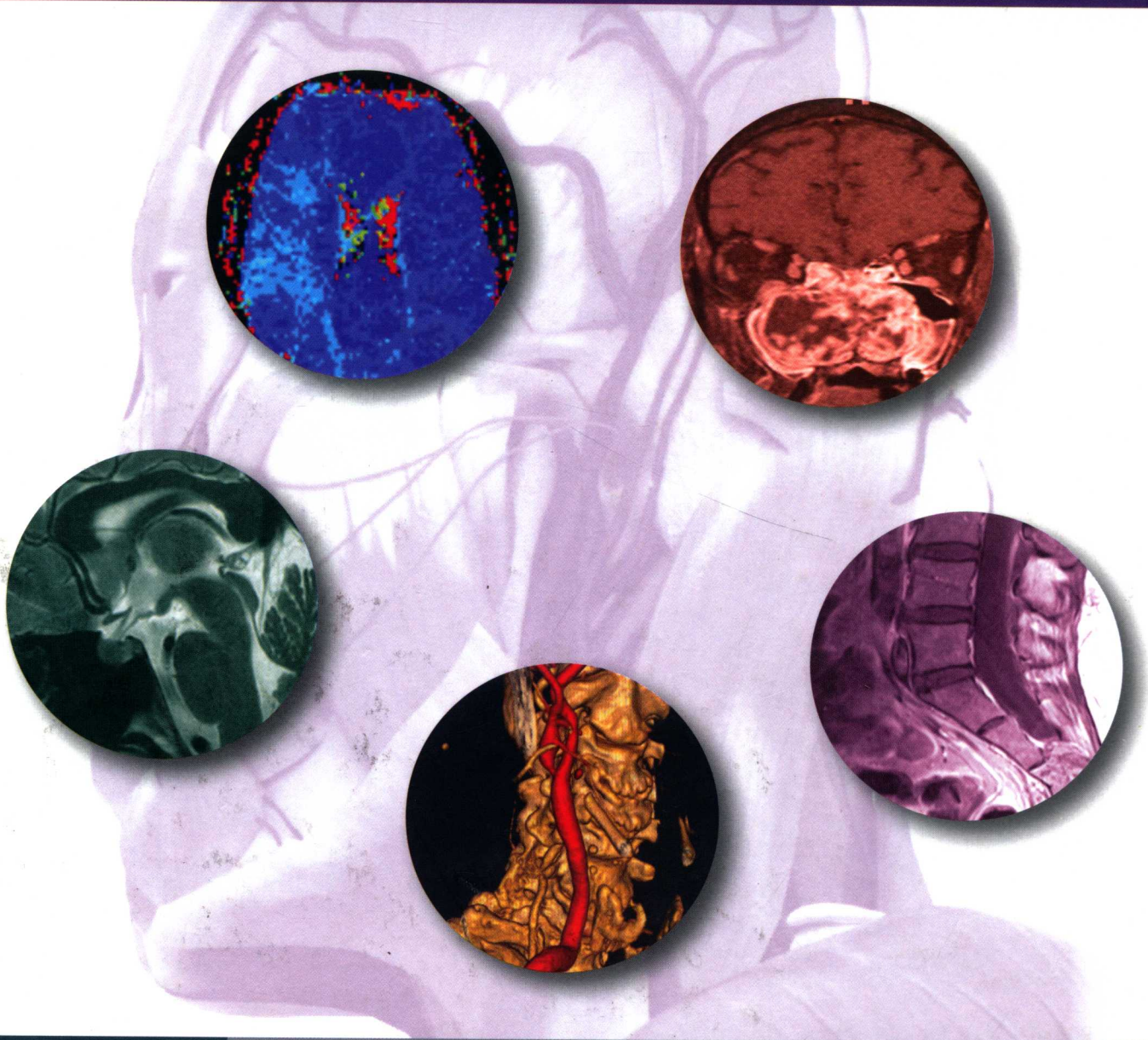


NAFI AYGUN, GAURANG SHAH, AND DHEERAJ GANDHI

Pearls and Pitfalls in

HEAD AND NECK AND NEUROIMAGING

Variants and Other Difficult Diagnoses



CAMBRIDGE

Medicine

Pearls and Pitfalls in HEAD AND NECK AND NEUROIMAGING

Variants and
Other Difficult
Diagnoses

Nafi Aygun

Associate Professor of Radiology and Director of the Neuroradiology Fellowship Program, Johns Hopkins University, Baltimore, MD, USA

Gaurang Shah

Associate Professor of Radiology, University of Michigan Health System, Ann Arbor, MI, USA

Dheeraj Gandhi

Professor of Radiology, Neurology and Neurosurgery at the University of Maryland School of Medicine, Baltimore, MD, USA



CAMBRIDGE
UNIVERSITY PRESS

CAMBRIDGE
UNIVERSITY PRESS

University Printing House, Cambridge CB2 8BS, United Kingdom

Published in the United States of America by Cambridge University Press, New York

Cambridge University Press is part of the University of Cambridge.

It furthers the University's mission by disseminating knowledge in the pursuit of education, learning and research at the highest international levels of excellence.

www.cambridge.org

Information on this title: www.cambridge.org/9781107026643

© Cambridge University Press 2013

This publication is in copyright. Subject to statutory exception and to the provisions of relevant collective licensing agreements, no reproduction of any part may take place without the written permission of Cambridge University Press.

First published 2013

Printed in Spain by Grafos SA, Arte sobre papel

A catalog record for this publication is available from the British Library

Library of Congress Cataloging in Publication data

Aygun, Nafi.

Pearls and pitfalls in head and neck and neuroimaging / Nafi Aygun, Gaurang Shah, Dheeraj Gandhi.

p. ; cm.

Includes bibliographical references.

ISBN 978-1-107-02664-3 (Hardback)

I. Shah, Gaurang. II. Gandhi, Dheeraj. III. Title.

[DNLM: 1. Neuroimaging--methods. 2. Central Nervous System Diseases--diagnosis.

3. Diagnosis, Differential. 4. Otorhinolaryngologic Diseases--diagnosis. WL 141.5.N47] RC349.D52

616.8'04754--dc23 2013010572

ISBN 978-1-107-02664-3 Hardback

Cambridge University Press has no responsibility for the persistence or accuracy of URLs for external or third-party internet websites referred to in this publication, and does not guarantee that any content on such websites is, or will remain, accurate or appropriate.

.....

Every effort has been made in preparing this book to provide accurate and up-to-date information which is in accord with accepted standards and practice at the time of publication. Although case histories are drawn from actual cases, every effort has been made to disguise the identities of the individuals involved. Nevertheless, the authors, editors and publishers can make no warranties that the information contained herein is totally free from error, not least because clinical standards are constantly changing through research and regulation. The authors, editors and publishers therefore disclaim all liability for direct or consequential damages resulting from the use of material contained in this book. Readers are strongly advised to pay careful attention to information provided by the manufacturer of any drugs or equipment that they plan to use.

Pearls and Pitfalls in
**HEAD AND NECK AND
NEUROIMAGING**

Variants and Other
Difficult Diagnoses

To my parents, Vrindavan and Vinu Shah, for their love and support;
my wife Kinnari, for taking the journey with me; and my sons Sharvil and Sahil,
for bringing joy into our lives.

Gaurang Shah

To Bobby, my best friend and life partner and for Shreya and Diya,
my beautiful daughters and the love of my life.

Dheeraj Gandhi

Preface

“A teacher is one who makes himself progressively unnecessary.”

– Thomas Carruthers

It is with a great sense of pride that we introduce our endeavor entitled *Pearls and Pitfalls in Head and Neck and Neuroimaging*. We hope that this book will be fun to read and foster the understanding of difficult diagnoses and common pitfalls in Neuroimaging.

We have different backgrounds and sub-specialty Neuroimaging expertise, but have one thing in common – the love and passion for teaching the residents and fellows. This has resulted in accumulation of thousands of teaching files in our respective libraries. Years spent with the trainees in the reading room in wonderful academic institutions have given us an understanding of diagnoses that are commonly missed and imaging findings that are likely to be misinterpreted.

While a number of excellent books exist on the subject and practice of Neuroradiology, a book like this is unique. It aims to cover the lacunae that commonly exist in the knowledge of Neuroimaging and gives clarity to diagnoses that are difficult to make with certainty.

After deciding to proceed with this project, the three of us brainstormed and came up with 106 topics that we wanted to cover. These topics were divided into 19 sections.

Each chapter is concise, yet gives a comprehensive overview of the subject matter.

We understand that time is precious and therefore wanted to create a resource that is precise and trustworthy. It is our hope that this treatise is easy to follow, unpretentious, and helpful.

We would like to thank all the Cambridge University Press staff who helped us tremendously every step of the way. In particular, we express our gratitude to Nisha Doshi and Beata Mako. Gaurang would also like to express his gratitude to Suresh Mukherji, Mark Shiroishi, Sanjay Jain, Prasan Rao, Jayant Narang and Mohammad Arabi for sharing their images and wisdom.

Our sincere thanks to the clinicians working with us for providing ever so important clinical feedback and learning that comes with it. Last but not the least, we thank our families for their unconditional support and patience during the writing of this project.

We hope that the readers will enjoy reading this book. We are open to any suggestions or criticism that the readers may have for its improvement and look forward to hearing from you.

Nafi, Gaurang, and Dheeraj

Contents

Preface ix

Section 1 Cerebrovascular diseases

- Case 1 Dense basilar artery sign 1
- Case 2 Global anoxic brain injury 4
- Case 3 Acute infarction 8
- Case 4 Vertebral artery dissection 10
- Case 5 Subacute infarct 13
- Case 6 Subarachnoid hemorrhage 17
- Case 7 Intracranial aneurysms 21
- Case 8 Giant aneurysms 23
- Case 9 Acute intracerebral hematoma 26
- Case 10 Cerebral amyloid angiopathy 30
- Case 11 Primary CNS vasculitis 34
- Case 12 Reversible cerebral vasoconstriction syndrome 37
- Case 13 Moyamoya disease/syndrome 40
- Case 14 Cortical venous thrombosis 43
- Case 15 Developmental venous anomalies 46
- Case 16 Dural arteriovenous fistula 49
- Case 17 Cavernous malformation 52

Section 2 Demyelinating and inflammatory diseases

- Case 18 Tumefactive demyelinating lesion 55
- Case 19 Acute disseminated encephalomyelitis 58
- Case 20 Progressive multifocal leukoencephalopathy 62
- Case 21 Osmotic myelinolysis 65
- Case 22 Neurosarcoidosis 72

Section 3 Tumors

- Case 23 Posterior fossa masses in children 80
- Case 24 Low-grade glioma 92
- Case 25 Diffuse intrinsic pontine glioma 105
- Case 26 Pseudoprogession of GBM 109
- Case 27 Pseudoreponse in treatment of GBM 112
- Case 28 Low-grade oligodendroglioma 114
- Case 29 Primary CNS lymphoma 116
- Case 30 Pineal region tumors 125
- Case 31 Intraventricular masses 140
- Case 32 Colloid cyst 153
- Case 33 Primary intraosseous meningioma 161
- Case 34 Suprasellar meningioma 171
- Case 35 Pituitary macroadenoma 180

Section 4 Infectious diseases

- Case 36 Brain abscess 191
- Case 37 Neurocysticercosis 194
- Case 38 Tuberculosis 198
- Case 39 Creutzfeldt–Jakob disease 207
- Case 40 Herpes encephalitis 210

Section 5 Metabolic and neurodegenerative conditions

- Case 41 Wernicke's encephalopathy 213
- Case 42 Hypertrophic olivary degeneration 217
- Case 43 Adrenoleukodystrophy 219

Section 6 Trauma

- Case 44 Mild traumatic brain injury 224
- Case 45 Isodense subdural hematoma 227

Section 7 Miscellaneous

- Case 46 Posterior reversible encephalopathy syndrome 229
- Case 47 Late-onset adult hydrocephalus secondary to aqueductal stenosis 232
- Case 48 Intracranial hypotension 234
- Case 49 Idiopathic intracranial hypertension 238
- Case 50 Rathke's cleft cyst 240

Section 8 Artifacts and anatomic variations

- Case 51 FLAIR sulcal hyperintensity secondary to general anesthesia 245
- Case 52 Virchow–Robin spaces 250
- Case 53 Arachnoid granulations 255
- Case 54 Benign external hydrocephalus 257
- Case 55 Pitfalls in CTA 260
- Case 56 Asymmetric pneumatization of the anterior clinoid process 264

Section 9 Skull base

- Case 57 Fibrous dysplasia of skull base 267
- Case 58 Sphenoid bone pseudolesion 271
- Case 59 Clival lesions 276
- Case 60 Perineural spread 282

Section 10 Temporal bone

- Case 61 Cochlear dysplasia 285
- Case 62 Labyrinthitis ossificans 289
- Case 63 Superior semicircular canal dehiscence 292
- Case 64 Fluid entrapment in the petrous apex cells 294
- Case 65 Acquired cholesteatoma 299
- Case 66 Malignant otitis externa 304
- Case 67 Temporal bone fractures 307

Section 11 Paranasal sinuses

- Case 68 Allergic fungal sinusitis 310
- Case 69 Invasive fungal sinusitis 316
- Case 70 Spontaneous CSF leaks and sphenoid cephaloceles 324
- Case 71 Juvenile nasal angiofibroma 328

Section 12 Orbits

- Case 72 Idiopathic orbital pseudotumor 331
- Case 73 Optic neuritis 336

Section 13 Salivary glands

- Case 74 Intraparotid lymph nodes 342
- Case 75 Benign mixed tumor 344
- Case 76 First branchial cleft cyst 350

Section 14 Neck

- Case 77 Nasopharyngeal cysts 354
- Case 78 Cystic nodal metastasis 357
- Case 79 Low-flow vascular malformations 360
- Case 80 Parapharyngeal masses 364

Section 15 Thyroid and parathyroid

- Case 81 Third branchial apparatus anomaly 370
- Case 82 Parathyroid adenoma 372
- Case 83 String sign 378

Section 16 Vessels

- Case 84 Carotid artery dissection 381
- Case 85 Traumatic arterial injury 384

Section 17 Spinal column

- Case 86 Craniovertebral junction injuries 387
- Case 87 Odontoid fractures 390
- Case 88 Vertebral compression fractures 398
- Case 89 Sacral insufficiency fracture 401
- Case 90 Paget's disease of the spine 405
- Case 91 Renal osteodystrophy 409
- Case 92 Calcific tendinitis of the longus colli 414

Section 18 Intervertebral discs

- Case 93 T2 hyperintense disc herniation 419
- Case 94 Disc herniation and cord compression 424
- Case 95 Postoperative disc herniation versus postsurgical scarring 427
- Case 96 Degenerative endplate alterations 430

Section 19 Spinal canal contents

- Case 97 Spinal dysraphism 434
- Case 98 Tethered spinal cord 445
- Case 99 Chiari I malformation 449
- Case 100 Spinal vascular malformations 455
- Case 101 Cord compression 458
- Case 102 Demyelinating/inflammatory spinal cord lesion 466
- Case 103 Subacute combined degeneration 469
- Case 104 Intradural cyst 471
- Case 105 Spinal CSF leaks 475
- Case 106 Leptomeningeal drop metastases 478

Index 486

Dense basilar artery sign

Imaging description

Intravascular clot can be seen on unenhanced CT as a focal hyperattenuation and may be the only sign of acute ischemia (Fig. 1.1). A thrombosed vessel has a higher CT attenuation value than a normal vessel, because clot contains more protein and less serum than blood due to the deposition of fibrinogen and other clotting proteins and extraction of serum during the process of thrombus formation. When CT shows a focal hyperattenuation in the middle cerebral artery (MCA) this is known as the dense MCA sign. This provides not only a diagnosis of MCA territory infarct but also some prognostic information, because stroke patients who demonstrate a dense MCA sign on their initial CT do relatively poorly compared to those who do not have this sign (Fig 1.2) [1]. Clot in the basilar artery is not as common as MCA thrombus, but the same principles that lead to the dense MCA sign apply to basilar artery thrombosis (Fig. 1.1) [2]. Similarly, thrombosis of the other intracranial vessels, including the veins and dural sinuses, can be diagnosed on the basis of dense clot present within the vessel (Figs. 1.3, 1.4).

Importance

Unenhanced CT is the first imaging study performed in most acute neurologic presentations. Diagnosing a vascular occlusion early has great prognostic significance. Early initiation of treatment is the most important factor in achieving improved outcomes in the setting of basilar occlusion [3].

Typical clinical scenario

MCA territory infarcts are relatively easy to diagnose clinically, as patients present with focal neurologic deficits and consciousness is usually not altered. Basilar artery territory infarcts, on the other hand, may lack localizing features and are associated with varying degrees of alteration in consciousness that require a broader clinical differential diagnosis than anterior circulation infarcts.

Differential diagnosis

Increased attenuation in a vessel can result from increased attenuation of the blood or the vessel wall in addition to intraluminal clot formation. Atherosclerosis results in focally increased attenuation in vessel wall that can mimic thrombus. Increased hematocrit due to hemoconcentration or systemic disorders such as chronic obstructive lung diseases may cause

diffusely hyperdense vessels that can potentially mimic the dense artery sign. Partial volume averaging, vessel tortuosity, or ectasia may also make a portion of the vessel appear denser than the other parts. Most of these possibilities can be eliminated by using thinner slices and comparing the vessel segment in question to other vessels of similar size on the same CT [4]. Of course, it is crucial to have appropriate clinical correlation. Contrast-enhanced CT/CTA or MRI/MRA can be used as a problem solver in ambiguous cases. It should be also kept in mind that the sensitivity of the dense vessel sign is relatively low. In other words, absence of dense artery sign does not exclude vessel occlusion or brain infarct.

Teaching points

The dense basilar artery sign indicates basilar artery thrombosis, basilar artery territory infarcts, and a poor outcome. In the appropriate clinical setting, the specificity of this finding is high although sensitivity is only moderate. Using thinner slices, comparing the density of the vessel in question to that of other vessels of similar size, helps to differentiate intraluminal clot from mimickers such as atherosclerosis, hemoconcentration, and vessel tortuosity. To confirm the presence of vessel occlusion, contrast-enhanced CT may be employed as a quick problem solving tool, although CTA, MRI/MRA, and sometimes digital subtraction angiography (DSA) are necessary to better characterize the extent of vessel occlusion, collateral vessels, and infarcted areas.

REFERENCES

1. Zorzon M, Masè G, Pozzi-Mucelli F, *et al.* Increased density in the middle cerebral artery by nonenhanced computed tomography: prognostic value in acute cerebral infarction. *Eur Neurol* 1993; **33**: 256–9.
2. Goldmakher GV, Camargo EC, Furie KL, *et al.* Hyperdense basilar artery sign on unenhanced CT predicts thrombus and outcome in acute posterior circulation stroke. *Stroke* 2009; **40**: 134–9.
3. Eckert B, Kucinski T, Pfeiffer G, Groden C, Zeumer H. Endovascular therapy of acute vertebrobasilar occlusion: early treatment onset as the most important factor. *Cerebrovasc Dis* 2002; **14**: 42–50.
4. Gadda D, Vannucchi L, Nicolai F, *et al.* Multidetector computed tomography of the head in acute stroke: predictive value of different patterns of the dense artery sign revealed by maximum intensity projection reformations for location and extent of the infarcted area. *Eur Radiol* 2005; **15**: 2387–95.

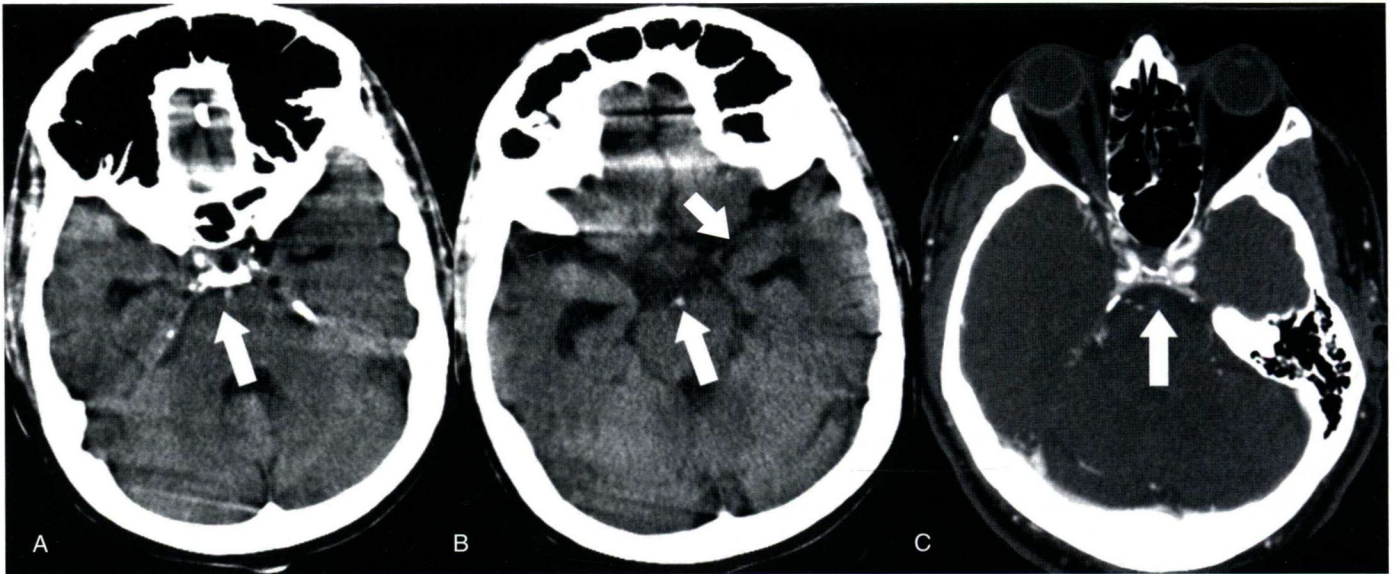


Figure 1.1 Acute basilar artery thrombosis. (A, B) Axial unenhanced CT images show increased attenuation in the basilar artery (arrows) as compared to the left middle cerebral artery (short arrow), indicating basilar artery thrombosis, in this patient with acute deterioration of neurologic status and alertness. (C) Axial image from a CTA performed shortly after shows lack of contrast filling of the basilar artery (arrow) compared to the carotids.

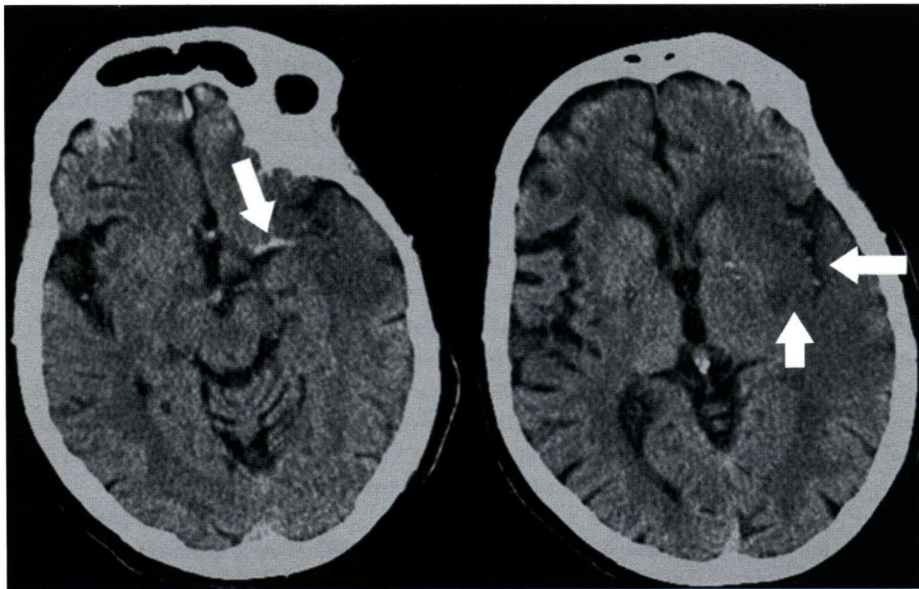


Figure 1.2 Axial CT images show increased attenuation associated with the left MCA and its branches (arrows) compatible with thrombosis. Decreased gray/white differentiation in the left insular ribbon and putamen (short arrow) is compatible with acute infarct.

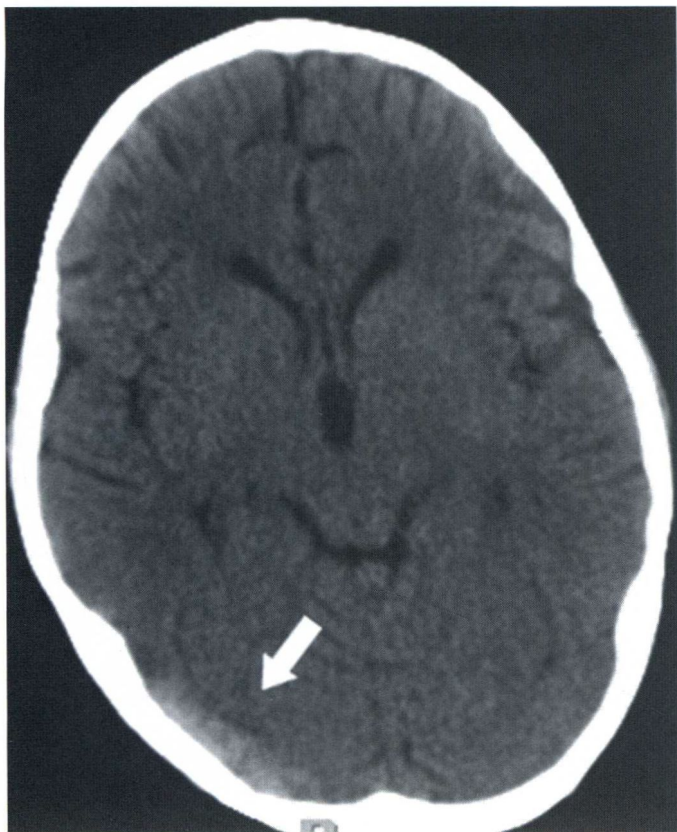


Figure 1.3 Axial CT shows a marked hyperattenuation in the right transverse sinus, which was confirmed to represent acute thrombosis.

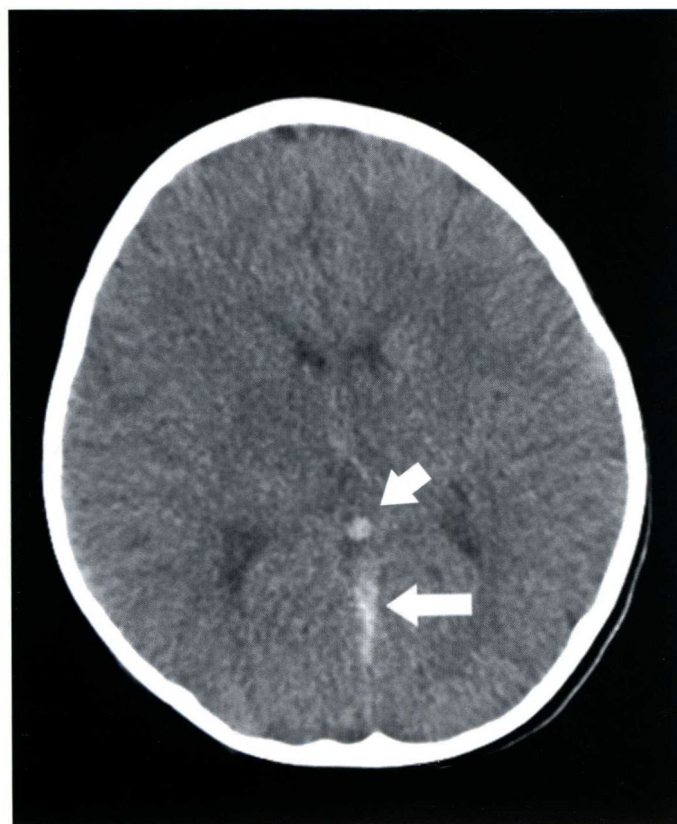


Figure 1.4 Axial CT shows thrombosis of the straight sinus (arrow) and the vein of Galen (short arrow) with associated hypoattenuation in the bilateral thalami.

Global anoxic brain injury

Imaging description

Anoxic–ischemic injury to the brain as a result of cardiorespiratory insufficiency, such as seen in cardiac arrest, respiratory arrest, prolonged hypotension, and asphyxia, is difficult to diagnose because of the subtlety and symmetry of abnormalities seen on MRI and CT scans. These scans are frequently misinterpreted, particularly when radiologists are not aware of the clinical circumstances. CT scans show diffuse decrease in gray/white differentiation and mild edema in the early stages. On MRI, diffuse increase in the cortical signal is seen on FLAIR/T2-weighted images as well as diffusion-weighted images (DWI) in most cases (Figs. 2.1, 2.2), although different patterns are occasionally encountered, including signal changes in the deep gray matter structures only, in both gray and white matter, and in the white matter only [1].

The underlying pathophysiologic processes leading to differences in pattern are not clearly understood, although essentially all types of global anoxic–ischemic injury portend a very poor prognosis. DWI sequence is the most sensitive imaging modality. DWI shows a much increased contrast difference between the diffusely abnormal cortex and relatively preserved white matter, creating a more “eye-pleasing” appearance compared to a normal DWI scan, which shows only a mild difference between gray and white matter (Fig. 2.3). However, there are differences in the normal contrast present between the cortex and white matter in different MRI scanners and different DWI sequences, and radiologists should become familiar with the normal appearance of the DWI images in their practice settings. High-b-value DWI may increase sensitivity [2].

Importance

Anoxic–ischemic injury, particularly when it is severe, often results in brain death, which has enormous implications for cessation of life support, family counseling, and organ harvesting.

Typical clinical scenario

Patients are typically comatose following cardiorespiratory arrest, prolonged hypotensive episode, asphyxia, drowning, etc.

Differential diagnosis

In the proper clinical setting there is no differential diagnosis. In strict radiological terms the differential diagnosis is between a normal scan and a severely abnormal scan, as missing this injury will result in generation of a normal MRI or CT report. One important clue is the difference in attenuation/signal of the supratentorial brain and cerebellum. Because the supratentorial structures are preferentially affected there is usually a stark difference between cerebellum and brain. When only the deep gray matter is involved (Fig. 2.4) the differential diagnosis may include Creutzfeldt–Jakob disease (CJD) and metabolic toxic injury, although the clinical features should be helpful in differentiating these. Only white matter involvement may be confused with leukoencephalopathies radiologically (Fig. 2.5).

Teaching points

Global hypoxic injury results in symmetric and subtle changes on MRI and CT scans that are easily missed. Radiologists should be familiar with the normal contrast present between the gray and white matter on their DWI sequences and look for changes in that contrast in comatose patients.

REFERENCES

1. Kim E, Sohn CH, Chang KH, Chang HW, Lee DH. Patterns of accentuated grey-white differentiation on diffusion-weighted imaging or the apparent diffusion coefficient maps in comatose survivors after global brain injury. *Clin Radiol* 2011; **66**: 440–8.
2. Tha KK, Terae S, Yamamoto T, *et al*. Early detection of global cerebral anoxia: improved accuracy by high-b-value diffusion-weighted imaging with long echo time. *AJNR Am J Neuroradiol* 2005; **26**: 1487–97.

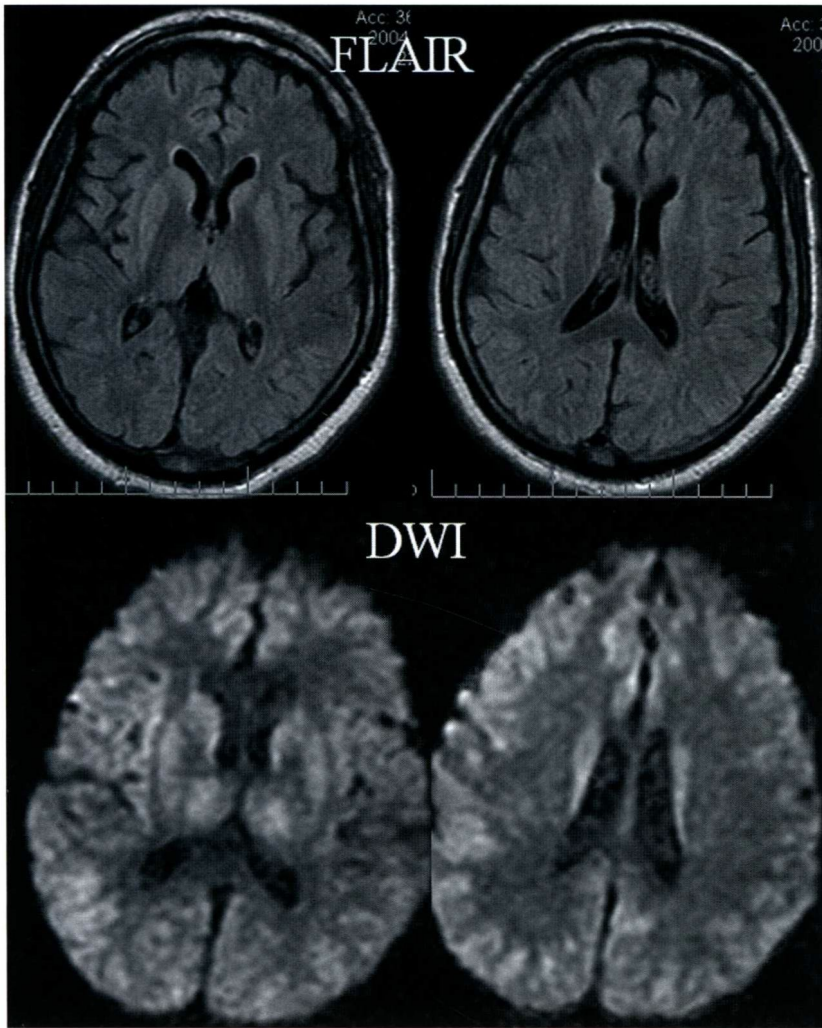


Figure 2.1 Axial FLAIR and DWI images show diffusely and symmetrically increased signal in the cortex and deep gray matter structures compatible with global anoxic injury. The patient had a cardiac arrest and was declared brain-dead shortly after the MRI.

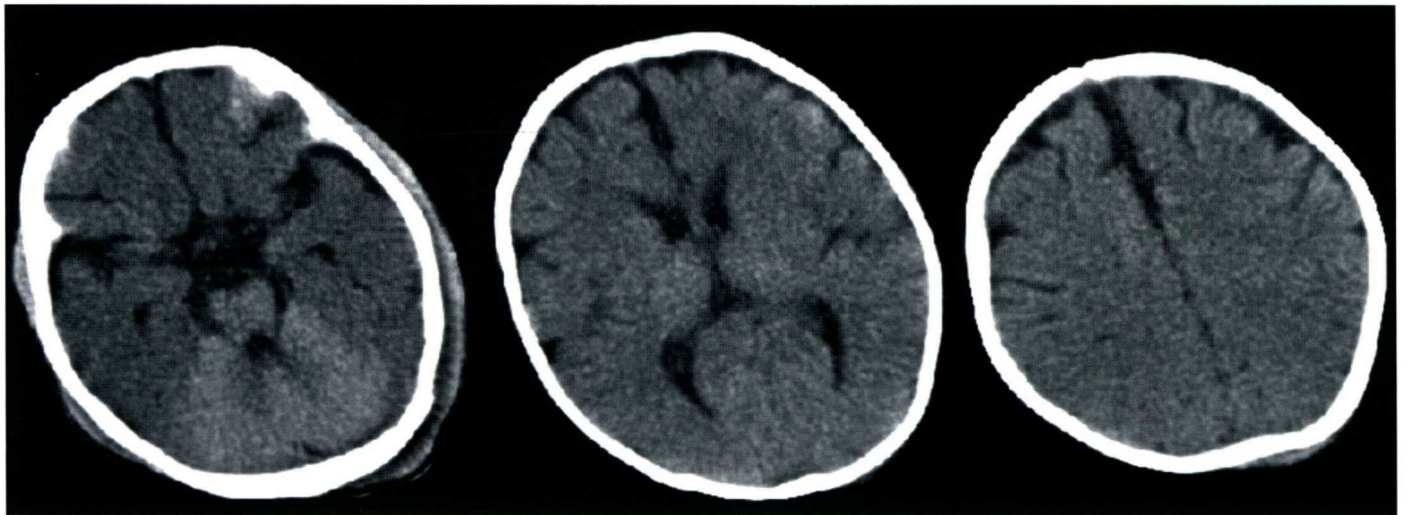


Figure 2.2 Axial CT images show diffuse loss of gray/white differentiation throughout the supratentorial brain compatible with global anoxic injury. Note the attenuation of the cerebellum, which appears prominent relative to diffusely decreased attenuation of the brain. This is the "white cerebellum sign." Similar differences are observed on MRI, in particular in DWI images.

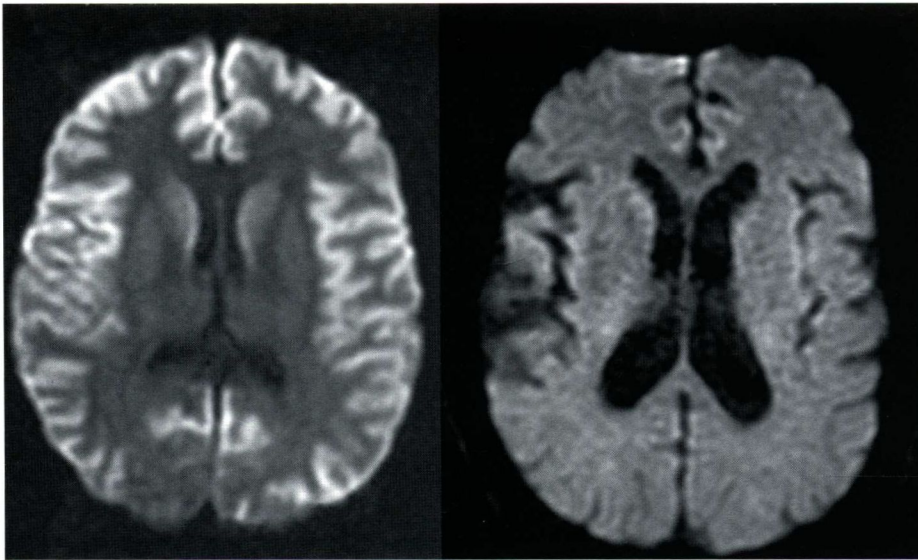


Figure 2.3 Axial DWI images of a patient with global anoxic injury (left) and of a normal individual (right) highlight the abnormality more clearly.

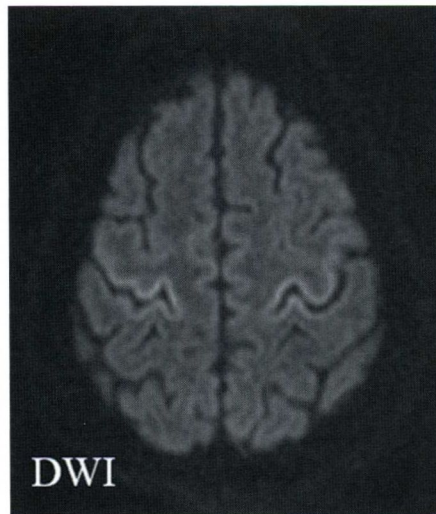
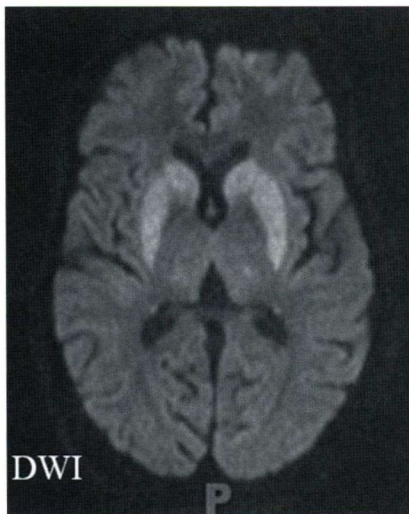
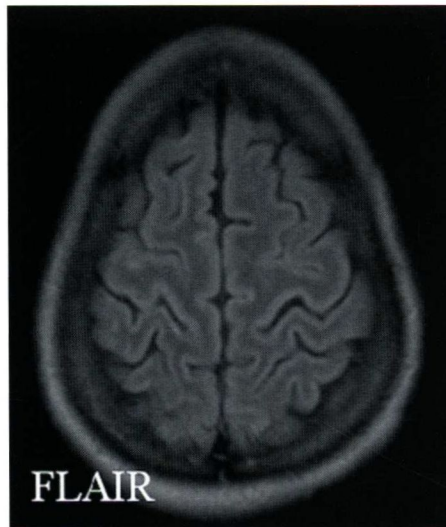


Figure 2.4 A less common pattern of global anoxic injury. Axial FLAIR and DWI images show preferential involvement of the deep gray matter with preservation of the cortex except in the perirolandic area.

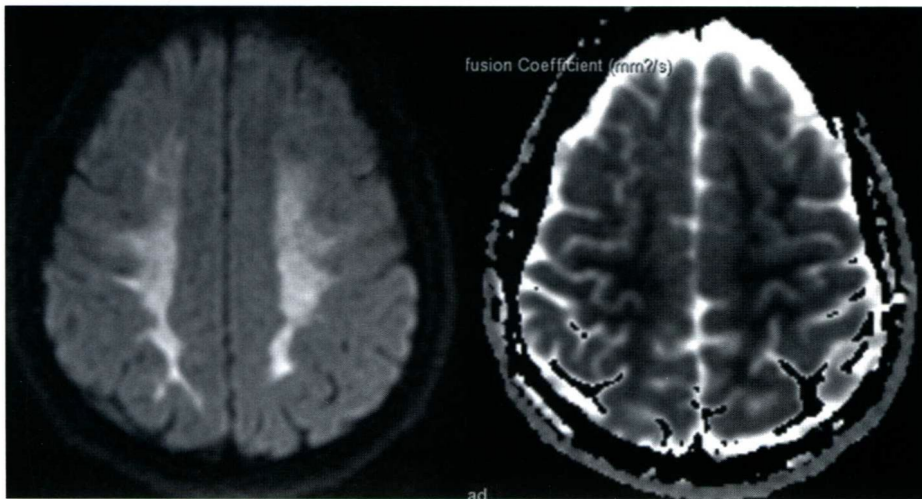


Figure 2.5 A much rarer form of global anoxic injury. White matter is involved and the cortex is spared, although quantitative apparent diffusion coefficient (ADC) evaluation showed some cortical abnormality as well.

Acute infarction

Imaging description

CT has an unparalleled track record in the detection of intracranial hemorrhage and therefore is the first imaging study obtained in this setting. In addition to excluding intracranial hemorrhage, CT may help demonstrate early signs of acute ischemic stroke (AIS), such as insular ribbon sign, hyperdense cerebral artery sign, sulcal effacement, and development of acute parenchymal low attenuation (Fig. 3.1). Patients who have advanced signs of infarction involving more than one-third of the middle cerebral artery (MCA) territory are generally excluded from intravenous tissue plasminogen activator (tPA) therapy because of a higher risk for hemorrhagic conversion.

Advanced imaging as a triage tool for selecting patients for intravenous (IV) or intra-arterial (IA) stroke therapies beyond 3 hours is a focus of evaluation of many ongoing clinical trials [1]. Central to the idea of advanced imaging is to obtain a precise measure of the area of ischemic core versus ischemic but still viable tissue that is at risk for infarction in the absence of early recanalization (penumbra). It can be argued that patients can only benefit from recanalization if there is a relatively modest area of already infarcted tissue and significant (ideally >20% of area of core infarction) ischemic tissue that can be potentially salvaged.

Ideally, imaging would provide an assessment (or confirmation) of occlusion of a major cerebral artery, a precise measure of the area of irreversible infarction, and assessment of the surrounding perfusion abnormality. MRI, using diffusion-weighted imaging (DWI), has become the gold standard to demonstrate the area of irreversible infarction. This tissue demonstrates high signal on DWI images and corresponding reduction in apparent diffusion coefficient (ADC) values. Salvageable penumbra can be operationally defined as a mismatch between the perfusion MR volume and the DW MR volume, where the perfusion MR volume indicates presumably ischemic, hypoperfused penumbral tissue and the DW MR volume represents irreversibly ischemic infarct core (Fig. 3.2).

CT imaging has its proponents, and they rely on a combination of CT angiography (CTA) (to demonstrate the vascular occlusion/cut-off) and CT perfusion (CTP). The area of irreversible infarction on CTP should demonstrate decrease in cerebral blood volume (CBV), and it can serve as a surrogate for DWI imaging. Similar to DWI–PWI mismatch,

investigators have used cerebral blood flow (CBF)–CBV mismatch or mean transit time (MTT)–CBV mismatch to assess the penumbral tissue on CTP, although the latter maps may be optimal (Fig. 3.3). However, CT has disadvantages of radiation exposure and, in institutions lacking 256- or 320-slice CTs, entire brain coverage is not possible. Post-processing is relatively more cumbersome, and thresholds vary based on post-processing techniques.

Importance

Radiologists must be familiar with early signs of stroke on CT as well as assessment of perfusion abnormalities in the setting of stroke.

Typical clinical scenario

Stroke is characterized by a sudden, acute neurologic deficit that is referable to the involved vascular territory. Common presentations include hemiparesis, facial droop, aphasia, and loss of consciousness, although a myriad of possible combinations of neurologic signs and symptoms are possible.

Differential diagnosis

With proper clinical correlation, imaging diagnosis of stroke is easily accomplished, especially on MRI. However, one must be alert to the possibility that there are numerous causes of restricted diffusion on DWI studies that need to be differentiated from acute stroke. Common causes of diffusion abnormalities other than stroke include encephalitis, traumatic lesions, acute demyelination, brain abscess, and highly cellular neoplasms.

Teaching points

Revascularization may be futile if there is no significant salvageable penumbral tissue (DWI–PWI mismatch). Moreover, such recanalization is potentially harmful, since it would restore blood flow to an already infarcted area.

REFERENCES

1. Köhrmann M, Schellinger PD. Acute stroke triage to intravenous thrombolysis and other therapies with advanced CT or MR imaging: pro MR imaging. *Radiology* 2009; 251: 627–33.

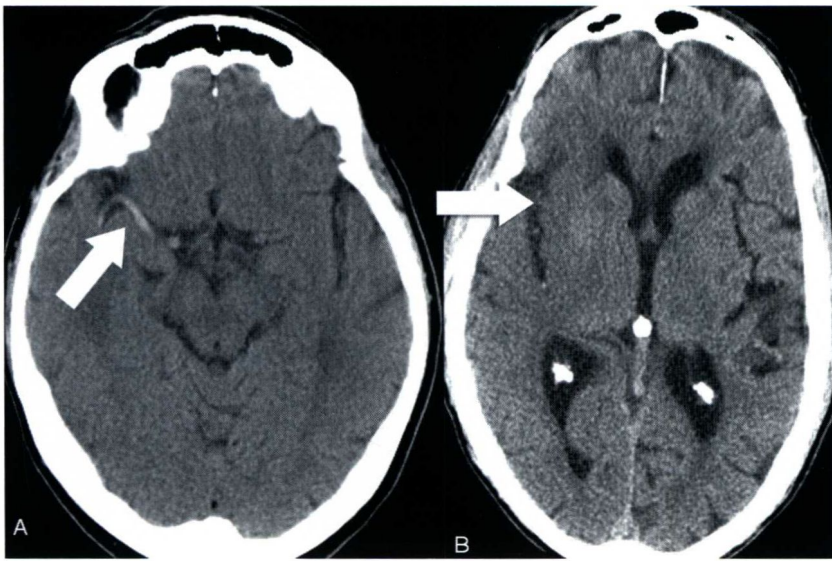


Figure 3.1 (A) Hyperdense middle cerebral artery (MCA) sign in a patient with acute left hemiparesis (arrow). (B) In another patient with acute stroke, the insular ribbon sign is noted (arrow). Additionally, the right-sided sulci are effaced and there is early parenchymal hypoattenuation, in comparison with the normal left side.

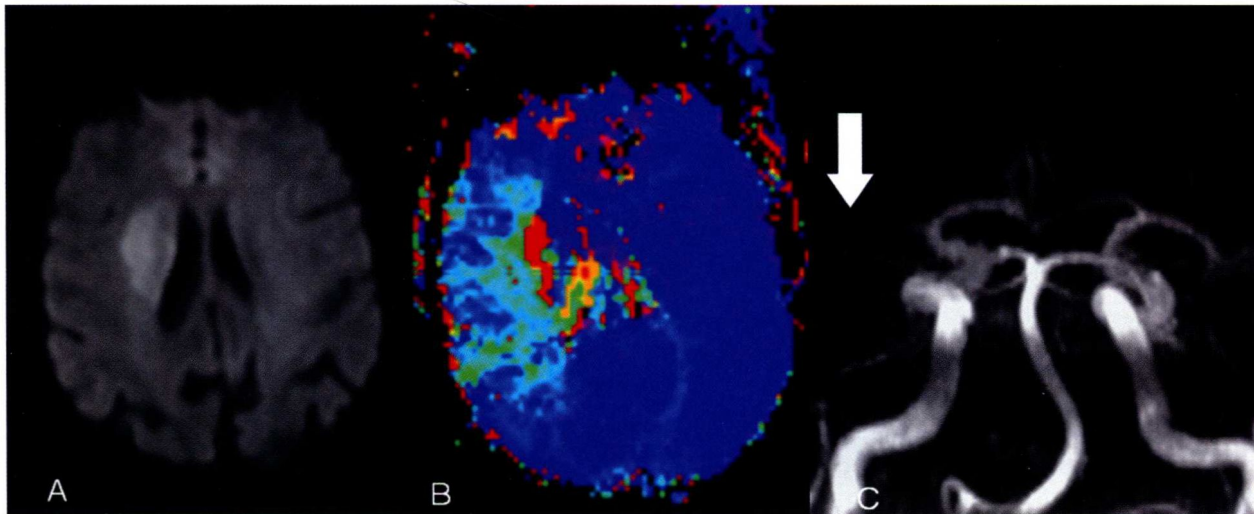


Figure 3.2 Utility of MRI as a trial tool for IA thrombolysis. (A) DWI, (B) PWI (MTT map), and (C) 3D time-of-flight (TOF) MRA are demonstrated in a patient with acute right MCA occlusion. Note a very small ischemic core on DWI, relatively large PWI defect, and occlusion of right M1 segment (arrow). This was successfully recanalized with IA thrombolysis, and neurologic deficits markedly improved.

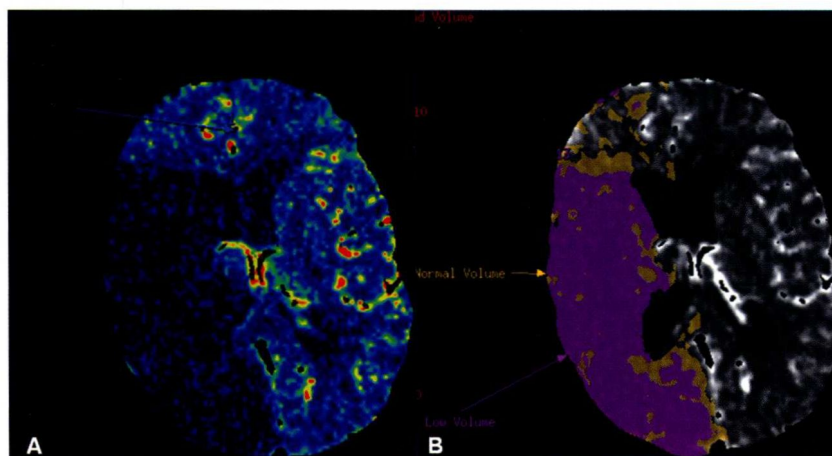


Figure 3.3 MCA ischemia of 90 minutes duration. (A) CBV map reveals an essentially completely infarcted right MCA and PCA territory. (B) A "penumbra" map. The purple area corresponds to CBV reduction and yellow areas highlight "penumbral tissue (MTT-CBV)." It would be futile to intervene in this patient because of lack of salvageable tissue.